Journal of Drug Delivery Science and Technology 102 (2024) 106399

Contents lists available at ScienceDirect

Journal of Drug Delivery Science and Technology

journal homepage: www.elsevier.com/locate/jddst

A preliminary investigation on hydrogel disks imbibed with enriched transfersomes as promising tool to promote the cutaneous deposition of vaccine antigens

Matteo Aroffu [a,c], Rita Abi Rached [a], Ines Castangia [a], Paola Italiani [b], Luciana D'Apice [b], Xavier Fernàndez-Busquets [h,i], Amparo Nacher [f,g], Maria Manconi [a,*], José Luis Pedraz [c,d,e], Maria Letizia Manca [a]

[a] Department of Scienze della Vita e dell'Ambiente, University of Cagliari, Cagliari, Italy
[b] Institute of Protein Biochemistry, National Research Council, Napoli, Italy
[c] NanoBioCel Group, Laboratory of Pharmaceutics, School of Pharmacy, University of the Basque Country (UPV/EHU), Vitoria-Gasteiz, Spain
[d] Biomedical Research Center in Bioengineering, Biomaterials and Nanomedicine (CIBER-BBN), Vitoria-Gasteiz, Spain
[e] BioAraba, NanoBioCel research Group, Vitoria-Gasteiz, Spain
[f] Department of Pharmacy and Pharmaceutical Technology and Parasitology, Pharmacy Faculty, University of Valencia, 46100, Valencia, Spain
[g] Instituto Interuniversitario de Investigación de Reconocimiento Molecular y Desarrollo Tecnológico (IDM), Universitat Politècnica de València, Av. Vicent Andrés Estellés s/n, Burjassot, 46100, Valencia, Spain
[h] Barcelona Institute for Global Health (ISGlobal, Hospital Clínic-Universitat de Barcelona), Rosselló 149-153, ES-08036, Barcelona, Spain
[i] Nanomalaria Group, Institute for Bioengineering of Catalonia (IBEC), The Barcelona Institute of Science and Technology, Baldiri Reixac 10-12, ES-08028, Barcelona, Spain

ARTICLE INFO

Keywords:
Phospholipid vesicles
Ovalbumin
Skin penetration
Hydrogel
Cling film
Franz vertical cells
Antigen presentation

ABSTRACT

The skin is an appealing and easily accessible route of administration for fast mass vaccination. However, it relies mainly on injection, meaning no immunization is achieved locally. In addition, pain, fear, and injuries strongly affect and reduce the effectiveness and adherence of patients to vaccination plans. Non-invasive routes of administration offer a safe and reliable solution. On these bases, three series of phospholipid vesicles were eco-friendly developed and adequately modified to pursue cutaneous immunization. Ovalbumin was selected as the model antigen, whereas transfersomes were chosen over liposomes because of their higher capability to cross the skin. Glycerol, sodium hyaluronate, or their combination were added to further improve their penetration, and this led to small (<60 nm), homogenous vesicles (polydispersity index <0.2), stable for up to 9 months. The colloidal formulations, alone or combined with occlusive strategies (achieved by cling film or hydrogel disks), were tested on tape-stripped skin to facilitate their application in a potential real-life context. While the enriched transfersomes alone provided better ovalbumin accumulation into the skin, the combination with cling film and especially with the hydrogel disks boosted their performance even further (using the hydrogel disks, in the epidermis, the ovalbumin accumulated ranged from ~30 to ~40 μg/cm^2 and in the dermis from ~4 to ~10 μg/cm^2). Despite the antigen-presenting assay do not show any immunogenicity for these vesicles ($p > 0.05$ with respect to the ovalbumin solution tested at the same dose), they are expected to perform better than the ovalbumin solution due to the protection and the enhanced skin deposition they provide. In addition, all the formulations can be safely administered as they are highly biocompatible in a wide range of doses (>100 % from 0.05 to 50 μg/mL of ovalbumin) and do not exert any inflammatory response. However, further studies are needed to confirm these promising preliminary results.

* Corresponding author.
E-mail address: manconi@unica.it (M. Manconi).

https://doi.org/10.1016/j.jddst.2024.106399
Received 20 July 2024; Received in revised form 9 October 2024; Accepted 7 November 2024
Available online 8 November 2024

1. Introduction

Vaccination represents one of the most significant discoveries in public health and thus one of the brightest chapters of human history, but it took a long time to catch on [1]. Historically speaking, it derives from a practice called "variolation" that spread across Africa, Asia, China, and the Ottoman Empire way before the 18th century, reaching Europe only at a later stage [2]. Fundamentally, it comprised the inoculation of small amounts of organic material into the skin, gathered from individuals who had contracted a disease, to prevent its onset [3]. The most famous case of variolation in Europe was related to smallpox and represents the foundation that ultimately led to the discovery of modern vaccination. Indeed, although variolation offered a pathway to establish robust immunity, the outcomes were unpredictable, making people either suffering from the disease they were supposed to avoid with the inoculation or even dying [4]. Only in 1798 did Edward Jenner manage to solve these problems with the inoculation of cowpox instead of smallpox, achieving the same effectiveness but with lower risks [2]. Since "cowpox" in Latin is "vaccinia", this injective procedure was renamed "vaccination" [4]. Nowadays, despite more than two centuries having passed since the first vaccination performed by Jenner, vaccines still rely on the injection of antigenic material into the human body, either intramuscularly, subcutaneously, or intradermally. As well known, several disadvantages are related to these invasive administration routes, such as pain, injuries, and fear, not to mention the high costs due to the disposal of the needles and the personnel training [5–9]. Considering these limitations, industries and researchers are now deeply committed to uncovering a solution. Non-invasive administration has emerged as an appealing strategy for mass vaccination and skin, which is easily accessible and hosts an immunologically rich environment, has gained importance once again [10]. Indeed, offering the possibility to elicit humoral, cellular, and even mucosal immune responses, it holds the potential to extend the application of conventional vaccines while allowing for dose reduction and improved complacency [11]. Unfortunately, the stratum corneum acts as the main skin physical barrier, making this route challenging to pursue [12]. Nanocarriers, due to their extremely small size, can improve the stratum corneum penetration making this route feasible [13]. Among the systems more frequently used, liposomes have found applications in several fields of modern medicine and are now exploited as powerful tools even in immunology [14,15]. The key to their success is mainly related to their lipidic, cell-like membrane structure surrounding an inner aqueous core, which allows them 1) to load hydrophilic, lipophilic, and even amphiphilic compounds, protecting them from degradation and the organism from its toxicity; 2) to be biocompatible and biodegradable due to their membrane composition; and 3) to allow the selective delivery to the targeted cell or tissue [16–23]. However, since the capability of conventional liposomes to cross the skin is limited, modified and improved vesicles have been developed [24]. Ultradeformable vesicles like transfersomes, for example, can increase the cutaneous penetration and retention of drugs after topical application, interacting with the skin temporarily and reversibly without generating any structural damage [25]. On these bases, Tyagi and colleagues developed a vaccine based on transfersomes successfully achieving immunization against a surface antigen of *Plasmodium falciparum* [26]. Rattanapak and co-workers, instead, undertook a comparative study of different nanocarriers (including transfersomes) under occlusive conditions, as these are believed to further increase skin penetration [27]. Lastly, Zhang et al. prepared antigen-loaded transfersomes and dispersed them in a PBS-ethanol gel to facilitate vaccine administration [28].

Bearing all these findings in mind, in the present study, transfersomes were developed and properly enriched with glycerol and/or hyaluronic acid to favour skin deposition of ovalbumin, which was loaded as a model antigen [29,30]. Tape-stripped skin was used in the *in vitro* studies because tape-stripping has been proven *in vivo* to enhance the production and release of cytokines, co-stimulatory molecules, and both humoral and cellular immune responses against peptide and DNA antigens upon topical application [31–33]. The carriers were directly applied upon non-occlusive or occlusive conditions or, alternatively, in enriched transfersome-imbibed hydrogel disks in order to achieve a proper cutaneous deposition of ovalbumin and to address one of the main drawbacks of colloidal systems: their permanence and adherence to the skin once applied. For the first time, the performances of water cosolvent-enriched transfersomes, applied in a non-occlusive or occlusive manner or imbibed into hydrogel disks, were compared to assess their efficacy in promoting the cutaneous deposition and retention of the model antigen. To conclude, their biocompatibility was evaluated on fibroblasts. A preliminary *in vitro* study of antigen presentation and inflammatory response was also performed using murine bone marrow-derived dendritic cells and human monocyte-derived macrophages.

2. Materials and methods

Lipoid S75 (phosphatidylcholine content: approximately 70 %) was purchased from AVG srl (Milan, Italy), whereas glycerol and sodium hyaluronate were sourced from Galeno (Carmignano, Italy). Vivaspin® 2 centrifugal concentrators (molecular weight cut-off: 100 kDa), Corning® syringe filters (cellulose acetate membrane, surfactant-free, diameter 28 mm, pore size 0.2 μm), ovalbumin (Grade VI, ≥98 %, Molecular Weight 45 kDa), sodium deoxycholate and all the other reagents of analytical grade were purchased from Sigma-Aldrich (Milan, Italy). Ultra-purified water (Milli-Q water) was obtained from a Milli-Q R4 system (Millipore, Italy) and used throughout the studies.

2.1. Preparation and purification of ovalbumin-encapsulated transfersomes

Ovalbumin-encapsulated transfersomes were eco-friendly produced by direct sonication, avoiding the use of organic solvent [34,35]. Specifically, Lipoid S75 (60 mg/mL), sodium deoxycholate (5 mg/mL), and ovalbumin (5 mg/mL) were dispersed in freshly prepared 0.9 % (w/v) saline (2 mL) containing glycerol (10 % w/v) or sodium hyaluronate (0.1 % w/v) or their combination at the same concentrations (Table 1). All the dispersions were sonicated four times (4 s on, 2 s off, 5 cycles, 14 μm amplitude) with a 5-min pause between each repetition to prevent overheating. Vivaspin® 2 centrifuge separators were used to remove the unencapsulated ovalbumin [36]. All the formulations were sterilized by filtration through Corning® syringe filters (pore size 0.2 μm) under a laminar flow hood and stored at 4 °C under vacuum in previously autoclaved vials.

2.2. Characterization of ovalbumin-encapsulated transfersomes

2.2.1. Morphological analysis

Cryogenic transmission electron microscopy was used to assess the formation of vesicles as well as their morphology. 5 μL of each colloidal dispersion were loaded on a glow-discharged holey carbon grid and blotted with filter paper to obtain a thin film. Vitrification was then performed on the film with a Vitrobot (FEI Company, Eindhoven, The Netherlands), submerging the grid (kept at 100 % humidity and room temperature) into ethane maintained at its melting point with liquid nitrogen. The obtained vitreous film was then transferred using a Gatan cryo-transfer (Gatan, Pleasanton, CA, US) to a Tecnai F20 TEM (FEI Company), and images of the samples were acquired at 200 kV, −175 °C and in low-dose imaging mode with a 4096 × 4096 pixel CCD Eagle camera (FEI Company) [37].

2.2.2. Physico-chemical properties

The Zetasizer Ultra (Malvern Instruments, Worcestershire, UK) was used to assess the mean diameter, polydispersity index, and zeta potential of the enriched transfersomes. The mean diameter (or average

Table 1
Qualitative and quantitative composition of ovalbumin-encapsulated enriched transfersomes.

	Lipoid S75 (mg/mL)	Sodium deoxycholate (mg/mL)	Ovalbumin (mg/mL)	Sodium hyaluronate (% w/v)	Glycerol (% w/v)	Saline solution (mL)
Glycerol-transfersomes	60	5	5	–	10	1
Hyaluronan-transfersomes	60	5	5	0.1	–	1
Glycerohyaluronan-transfersomes	60	5	5	0.1	10	1

hydrodynamic diameter) of vesicles and polydispersity index, which is the width of their size distribution, were determined on the basis of dynamic light scattering. This non-invasive technique measures the intensity fluctuations of the light scattered by particles in suspension, allowing to calculate the velocity of their Brownian motion and thus their size according to the Stokes-Einstein relation. Zeta potential, which represents a measure of the extent of electrostatic repulsion or attraction between particles, was determined by measuring the electrophoretic light scattering as it relates the velocity of the particles towards the oppositely charged electrode (electrophoretic mobility) to their net charge. Sample preparation before analysis was carried out in a sterile environment under a laminar flow hood. All samples were measured at a scattering angle of 175° (back-scatter) [38]. Before the analysis, all samples were diluted with water to obtain optically clear dispersions, thereby avoiding attenuation of the laser beam and reducing detectable scattered light, in accordance with the producer's recommendations [39]. Different dilutions (from 1:10 to 1:1000) were preliminarily tested; following the intelligent data quality advice provided by the ZX software, the 1:100 dilution was selected for the experiments, as it ensured more adequate count rates and reproducibility.

2.2.3. Long term stability

Sterilized formulations were stored at 4 °C and kept under vacuum before and after every measurement. Mean diameter, polydispersity index, and zeta potential were assessed with the Zetasizer Ultra (Malvern Instruments, Worcestershire, UK) at regular intervals for 9 months in order to detect any variation. Sterility was maintained throughout the assessment, working under a laminar flow hood.

2.2.4. Stability after freeze-thawing and freeze-drying

Mean diameter and polydispersity index were measured with the Zetasizer Ultra (Malvern Instruments, Worcestershire, UK) after freeze-thawing and freeze-drying to evaluate their stability during these processes.

2.2.5. Encapsulation efficiency

Vivaspin® 2 centrifugal separators were used to separate the unencapsulated ovalbumin from vesicle dispersions. Each enriched transfersome was diluted (1:10 v/v) in its respective media to achieve a concentration of 6 mg/mL of Lipoid S75 and 0.5 mg/mL of ovalbumin, transferred in the centrifugal separators and centrifuged at 1000 rpm for 2 h, at 25 °C, using a centrifuge equipped with swing bucket rotor. The free ovalbumin was collected from the purification filtrates and analyzed with the bicinchoninic acid protein assay kit (Novagen®) [40]. According to the manufacturer's instructions, the absorbance was measured at $\lambda = 562$ nm with a UV spectrophotometer (Lambda 25, PerkinElmer, Milan, Italy). All experiments were performed in triplicate.

2.3. Preparation and characterization of hydrogel disks

Hydrogel was prepared by dispersing polyvinyl alcohol (10 % w/v) in Milli-Q water and sonicating system (4 s on, 2 s off, 90 cycles, 14 μm amplitude) to obtain a clear dispersion and avoid bubble formation. Aliquots (300 μL) of dispersions were poured into each well of a 24-well plate, frozen at −20 °C for 16 h, and thawed for 8 h (freeze-thawed). After two freeze-thaw cycles, samples were freeze-dried at 0.5 mBar for 8 h after freezing samples (−20 °C) overnight with no additional secondary drying. Finally, all hydrogels were cut round with a chisel (hydrogel disks).

2.3.1. Swelling ratio and imbibition time of hydrogel disks

The ability of the hydrogel disks to capture water (swelling) over time was measured as a function of weight changes. Therefore, the freeze-dried hydrogel disks (n = 3) were weighted on an analytical balance, submerged in an excess of water (9 mL), and, at each time point (0.5, 1, 2, 3, 4, 6, and 8 h), they were gently blotted with paper, reweighted, and submerged in water again, noting the weights. The hydrogel disk swelling (%) was calculated on the basis of the weight of the freeze-dried hydrogel, whereas the equilibrium swelling and the time needed to reach it (minimum imbibition time) were determined once a constant hydrogel disk weight was achieved after repeated submersion in water [41].

2.3.2. Loading of labeled ovalbumin dispersions into hydrogel disks and analysis of their contents

Freeze-dried hydrogel disks (n = 3) were hydrated with 300 μL of labeled ovalbumin in solution or encapsulated in transfersomes and incubated for 3 and 12 h within a 24-well plate. At each time point, each hydrogel disk was taken, placed in an amber vial (10 mL) with 2.7 mL of water, and sonicated (4 s on, 2 s off, 40 cycles, 14 μ amplitude) to release vesicles. Subsequently, 10 μL were withdrawn, diluted with 2.49 mL of a mixture of ethanol and methanol (1:1 v/v), and sonicated to release labeled ovalbumin from the enriched transfersomes. A centrifugation cycle (4000 rpm, 10 min, 25 °C) was performed in order to deposit any debris before reading the fluorescence of the supernatant (190 μL) with a plate reader (Lambda 25, PerkinElmer, Milan, Italy).

2.4. In vitro characterization of ovalbumin-encapsulated transfersomes

2.4.1. Penetration studies

To facilitate the quantification of ovalbumin content and deposition in the deepest skin layers (epidermis and dermis), it was conjugated with fluorescein isothiocyanate according to the protocol developed by Ahmed et al. and the enriched transfersomes were prepared by replacing ovalbumin with the labeled ovalbumin [42].

In vitro deposition studies were performed using vertical Franz cells with an effective diffusion area of 0.785 cm^2, thermostated at 37 ± 1 °C, and maintained under continuous magnetic stirring (300 rpm). The excised dorsal skin of one-day-old pigs (~1.5 kg) dead from natural causes, provided by a local slaughterhouse, were defrosted, stripped to remove stratum corneum by adhesive tape Tesa® AG (Hamburg, Germany) (n = 10 strips) and sandwiched between the donor and receptor compartments of the cells. To evaluate the integrity of the skin, 1 mL of phenol red solution (0.5 mg/mL) was applied onto the skin surface in the donor compartment and quantified in the receptor compartment spectrophotometrically [43]. For the penetration studies, the receptor compartment was filled with saline solution (5.5 mL) avoiding any bubble formation, and the skin specimens (n = 6 per formulation) were left to equilibrate at 37 ± 1 °C in this solution overnight. 100 μL of labeled ovalbumin (corresponding to 500 μg of labeled ovalbumin), in solution or encapsulated in the enriched transfersomes, was applied onto the skin specimen in non-occlusive or occlusive conditions, the

latter achieved with cling film. Alternatively, the hydrogel disks previously imbibed with the same samples were also applied to the skin. To detect autofluorescence, labeled ovalbumin was replaced by saline solution (100 μL), and skin specimens treated under the same conditions (non-occlusive or occlusive conditions achieved by cling film or hydrogel disks) were used as control. The Franz cells were covered with tin foil to avoid direct exposure to light. Every 2 h, the saline solution was withdrawn and replaced by a new medium to mimic the sink conditions. Experiments were conducted for 4 and 8 h, and, in the end, the epidermis and dermis were severed and sliced using a surgical scalpel. As reported elsewhere, this type of separation is suitable for any situation, and it is made possible by the difference in the visual aspects of the two layers (the epidermis is dark while the dermis is white) [44,45]. Severed and sliced epidermis and dermis were placed in amber glass vials with 2 mL of a mixture of ethanol and methanol (1:1 v/v) and sonicated in an ice bath to extract the free labeled ovalbumin. The resulting solution was filtered with syringe filters (Corning® pore size 0.2 μm), and the ovalbumin was fluorescently quantified (excitation: 495 nm; emission: 520 nm) with a multiple reader (Lambda 25, PerkinElmer, Milan, Italy).

2.5. Biocompatibility assay

Fibroblasts L929 cells were grown in monolayers under standard conditions (37 °C, humidified, 5 % CO_2), using Dulbecco's Modified Eagle Medium (DMEM) supplemented with foetal bovine serum (10 % v/v), penicillin (100 U/mL), and streptomycin (100 μg/mL). Biocompatibility assay was carried out according to the *in vitro* methods for cytotoxicity assessment included in ISO 10993-5 [46]. Briefly, fibroblast L929 cells were seeded at a density of 1×10^5 cells/mL in 96-well plates (100 μl/well) and incubated under standard conditions for 24 h. The complete medium was then replaced with medium-diluted formulations (glycerol-transfersomes, hyaluronan-transfersomes, and glycerohyalur onan-transfersomes) or ovalbumin solution at different ovalbumin concentrations (0.05, 0.5, 50, and 500 μg/mL). After an additional incubation period (24 h), the supernatant was removed, 100 μL of 3-(4, 5-dimethylthiazole-2-yl)-2,5-diphenyltetrazolium (MTT, 0.5 mg/mL) were added, and the formazan formation was determined for each concentration tested after crystals dissolution in DMSO and compared to that determined in culture controls. The absorbance was read at 570 nm with a microplate reader (Lambda 25, PerkinElmer, Milan, Italy).

2.6. Culturing of bone marrow-derived dendritic cells and B3Z cells

Bone marrow derived dendritic cells were obtained from precursors isolated from the tibiae of euthanized eight-week-old, female, C57BL/6 mice (Charles River, Lecco, Italy) that had been housed in pathogen-free conditions, in accordance with institutional guidelines. The experiments were performed following the EU Directive 2010/63/EU for animal experiments and were authorized by the Italian Ministry of Health with the authorization number 7E58D.12 released on 5-20-2020. Tibiae were deprived of their extremities, and the contained marrow was washed with ice-cold RPMI 1640 medium. Cells were resuspended by pipetting, washed twice with medium, seeded, and cultured with recombinant murine granulocyte/macrophage colony-stimulating factor (200 U/mL) in RPMI 1640 medium supplemented with 10 % foetal calf serum, 60 μg/mL penicillin, 100 μg/mL streptomycin, 1 mM sodium pyruvate and 50 μM 2-mercaptoethanol. After 8 days, immature dendritic cells were collected and used in the antigen presentation assay.

B3Z cells (OT-I hybridoma line) were used as they specifically recognize the ovalbumin octapeptide (257–264) SIINFEKL exposed on the major histocompatibility complex I (MHC I) of the surface of dendritic cells, allowing the production of interleukin-2 in response. These cells were grown in complete RPMI 1640 medium (10 % foetal calf serum, 100 U/mL penicillin, 100 μg/mL streptomycin, 1 % glutamine, 1 % non-essential amino acids, 1 % sodium pyruvate and 50 μM 2-mercaptoethanol) and co-cultured with bone marrow-derived dendritic cells for the antigen presentation assay [47].

2.6.1. Antigen presentation assay and interleukin-2 detection

Bone marrow-derived dendritic cells (1×10^6/mL) were incubated overnight with different concentrations of ovalbumin in solution or loaded in the enriched transfersomes (1–5 μg/mL). A blank control was made incubating cells with only medium. Subsequently, the bone marrow-derived dendritic cells were co-cultured with B3Z cells (OT-I hybridoma line, 5×105/well) for 40 h, and the amount of interleukin-2 released into supernatants was assessed as a measure of uptake and processing of ovalbumin (ovalbumin-peptide 257–264). From each well, 100 μL of supernatant was analyzed in duplicate using a mouse IL-2 ELISA MAX Standard kit in two independent experiments, according to the manufacturer's instructions.

2.7. Human monocyte isolation and culturing of monocyte-derived macrophages

Discarded buffy coats of healthy blood donors were used, upon informed consent, to obtain monocytes. Briefly, Ficoll-Paque gradient density separation was adopted to separate human peripheral blood mononuclear cells, while magnetic microbeads allowed for the isolation of monocytes by CD14 positive selection according to the manufacturer's instructions (Miltenyi Biotec, Bergisch Gladbach, Germany). Only >95 % viable and pure monocytes (determined by trypan blue exclusion and cytosmears) were used in the experiments. Monocytes were grown in RPMI 1640 + Glutamax-I medium supplemented with 50 μg/mL of gentamicin sulfate, 5 % heat-inactivated human AB serum, and 10 ng/mL of human recombinant M-CSF. Differentiation in macrophages was achieved by incubating cells at 37 °C in 5 % CO_2 for 7 days and replacing the medium every 3 days.

2.8. Biocorona formation on transfersome surface

Before the stimulation of monocyte-derived macrophages, glycerol-transfersomes, hyaluronan-transfersomes, and glycerohyaluronan-transfersomes were admixed 1:1 (v/v) with heat-inactivated serum and incubated for 1 h at 37 °C in an orbital shaker at 300 g to allow the formation of the serum protein biocorona on vesicles' surface and ensure their stability in culture. The serum pre-coated transfersomal vesicles were added directly to the culture plates, and their concentration was adjusted to the desired values for each treatment based on the amount of ovalbumin.

2.9. Stimulation of monocyte-derived macrophages and detection of tumor necrosis factor-α

Monocyte-derived macrophages were incubated overnight with different concentrations of ovalbumin in solution or loaded in enriched transfersomes (0.2, 1, and 5 μg/mL, final concentrations). Incubation with only medium and medium-diluted lipopolysaccharide (10 ng/ml) were used as negative and positive control, respectively. At the end of the experiments, supernatants were collected, centrifuged, and frozen at −80 °C before cytokine analysis. The amount of tumor necrosis factor-α in the culture supernatants was measured by a human TNF-α ELISA kit using a MultiScan FC reader (ThermoScientific), according to the manufacturer's instructions. Results are reported as mean ± standard deviation of values from 2 replicate samples from the same donor.

2.9.1. Statistical analysis of data

Results are expressed as the mean ± standard deviation. Statistically significant differences among samples were determined by using variance analysis. The post-hoc Tukey-Kramer *t*-test was used to substantiate significant differences between the means of two specific groups. The statistical analysis was performed using the Excel software package

(Microsoft Corp, Redmond, USA) equipped with a tool for statistical analysis. The minimum level of significance chosen was $p < 0.05$.

3. Results

3.1. Characterization of ovalbumin-encapsulated enriched transfersomes

The mean diameter, polydispersity index, zeta potential, and entrapment efficiency of ovalbumin-encapsulated enriched transfersomes were measured (Table 2). All the vesicles were sized <60 nm and homogeneously dispersed, as the polydispersity index was ≈0.2. Hyaluronan-transfersomes had a slightly larger mean diameter (~57 nm) than glycerol-transfersomes and glycerohyaluronan-transfersomes. The larger diameter of hyaluronan-transfersomes might be due to the electrostatic and hydrophobic interactions that occur between phosphatidylcholine and hyaluronic acid, as reported elsewhere [48]. On the other hand, the addition of glycerol to the mixture is well known to increase deformability and flexibility, which might be partially responsible for the formation of smaller vesicles thus masking the interaction effect between phosphatidylcholine and hyaluronic acid [49]. The differences were also confirmed by cryogenic electron microscopy (Fig. 1). Along with size, morphology was affected by the composition of the hydrating medium: glycerol, sodium hyaluronate or their combination. Specifically: glycerol-transfersomes were small and had irregular and elongated shapes; hyaluronan-transfersomes were larger and more spherical; glycerohyaluronan-transfersomes were smaller, completely spherical, and uniformly sized. Neither the strongly negative zeta potential (~-32 mV, $p > 0.05$ among the 3 values) nor the encapsulation efficiencies (~63 %, $p > 0.05$ among the 3 values) were significantly affected by the hydrating phase. The strong negative charge on the transfersome surface was likely due to S75, which is a mixture of phosphatidylcholine, negatively charged phospholipids, and fatty acids [20]. A strong negative charge, < - 30 mV, and a narrow polydispersity index, <0.3, are believed to provide safer, and more stable and efficient nanocarriers [50,51].

Variations of mean diameter, polydispersity index, and zeta potential were monitored over time, every 3 months for 9 months, to evaluate the stability of the ovalbumin-encapsulated transfersomes once stored at 4 °C and under vacuum. All the vesicle dispersions were stable for 9 months of study, with no need to add any preservative or stabilizer (Fig. 2). Comparing the mean diameters of fresh formulations with their respective mean diameters after 1, 3, 6 and 9 months, no significant differences were detected as glycerol-transfersomes, hyaluronan-transfersomes and glycerohyaluronan-transfersomes retained their initial hydrodynamic diameter <60 nm ($p > 0.05$ among the values of each sample). Similarly, zeta potential did not undergo significant variations over time, remaining constant (~-32 mV, $p > 0.05$ among the values of each sample).

Table 2
Mean diameter (MD), polydispersity index (PI), zeta potential (ZP), and entrapment efficiency (EE) of ovalbumin-encapsulated enriched transfersomes. The same symbols (*, °, ^, #) indicate values that are not statistically different ($p > 0.05$), while different symbols indicate significant differences ($p < 0.05$). Mean values ± standard deviations, obtained from at least 3 measurements, are reported.

	MD (nm)	PI	ZP (mV)	EE (%)
Glycerol-transfersomes	50 ± 1*	0.21 ± 0.01°	−29 ± 2^	65 ± 7#
Hyaluronan-transfersomes	57 ± 2*	0.22 ± 0.01°	−34 ± 9^	61 ± 6#
Glycerohyaluronan-transfersomes	49 ± 3*	0.20 ± 0.01°	−30 ± 6^	64 ± 5#

3.2. Stability of transfersomes after freeze-thawing and freeze-drying

Since the enriched transfersomes were intended to be loaded into hydrogel disks, their stability was evaluated after freeze-thawing and freeze-drying, as they were both steps required to prepare the hydrogel disks. Thus, after these processes, the mean diameter and polydispersity index of the enriched transfersomes were measured again (Fig. 3). A significant increase in the size was found for all the formulations since the first cycle of freeze-thaw, as the mean diameter of hyaluronan-transfersomes changed from ~57 to ~92 nm ($p \ll 0.05$), and that of glycerohyaluronan-transfersomes from 49 to ~100 nm ($p \ll 0.05$). This increase in size was remarkably higher if compared with that of glycerol-transfersomes, whose mean diameter increased only from ~50 to ~70 nm. Interestingly, the second cycle did not further significantly affect the mean diameters, suggesting that, after a possible initial rearrangement of the double bilayer, all these vesicles are unaffected by subsequent freeze-thaw cycles. After freeze-drying, the mean diameter changed again, especially that of glycerol-transfersomes (from ~70 to ~370 nm), while glycerohyaluronan-transfersomes underwent less variation (from ~98 to ~192 nm). The polydispersity index of glycerol-transfersomes and glycerohyaluronan-transfersomes changed drastically from initial values of ~0.20 to final values of ~0.38, whereas that of hyaluronan-transfersomes remained unchanged (~0.23) indicating that the newly arranged vesicles were homogeneously dispersed.

Overall, freeze-thawing and freeze-drying strongly affected the physicochemical properties of all the enriched transfersomes. Consequently, hydrogel disks were imbibed with the enriched transfersomes only after they had been prepared by freeze-thawing and freeze-drying.

3.3. Characterization of hydrogel disks and imbibition with ovalbumin in solution or encapsulated in enriched transfersomes

Since the preparation steps of the hydrogels (freeze-thaw and freeze-dry) had a strong negative impact on the physicochemical properties of the enriched transfersomes (Fig. 3), empty freeze-dried hydrogel disks were firstly prepared and after imbibed with formulations. Their ability to capture water was evaluated to identify the imbibition time, and the swelling ratio at different time points (0.5, 1, 2, 3, 4, 6, and 8 h) was calculated (Table 3). The time needed to reach the equilibrium was found allowing to select the minimum incubation time needed to imbibe the hydrogel disks (minimum imbibition time) completely. After submerging the freeze-dried hydrogel disks in water for 0.5 h, their swelling ratio hugely increased up to ~391 % compared to the initial value (Table 3). Subsequent increases were detected at 1, 2, and 3 h. From 3 h onwards, there were no statistical differences among the swelling ratios (≈418 %, $p > 0.05$ between the values at 3, 4, 6, and 8 h). Consequently, 3 h was identified as the minimum imbibition time to completely imbibe the hydrogel disks with ovalbumin solution or ovalbumin-encapsulated enriched transfersomes in the next studies.

To confirm the effectiveness of the minimum imbibition time, empty freeze-dried hydrogels were allowed to imbibe with labeled ovalbumin in solution or encapsulated in transfersomes for 3 or 12 h. The amount of ovalbumin was quantified (Table 4). No statistical differences were found in the ovalbumin content among the hydrogel disks with respect to the time points (3 or 12 h) or the formulations tested (solution, glycerol-transfersomes, hyaluronan-transfersomes or glycerohyalur onan-transfersomes), as it was always ~22 % ($p > 0.05$ among the different values, correspondent to ~330 μg of ovalbumin per disk). Thus, according to the swelling study, 3 h were enough to achieve the complete imbibition of the hydrogel disks also with the labeled ovalbumin in solution or encapsulated in the enriched transfersomes.

3.4. In vitro penetration studies

The capability of labeled ovalbumin (500 μg) in solution or encapsulated in enriched transfersomes to penetrate in the tape-stripped skin

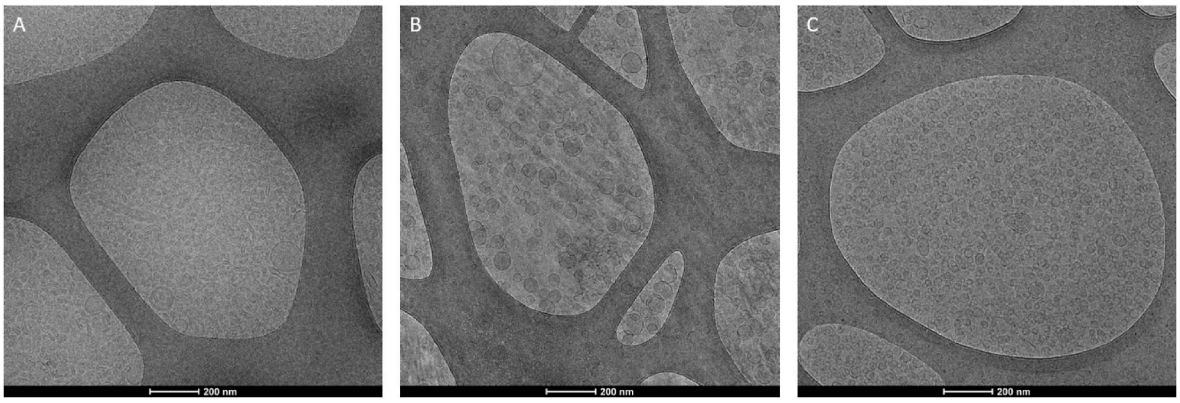

Fig. 1. Representative cryogenic transmission electron microscopy images of glycerol-transfersomes (A), hyaluronan-transfersomes (B), and glycerohyaluronan-transfersomes (C).

Fig. 2. Stability over time evaluated by measuring mean diameter (upper panel, bars), polydispersity index (upper panel, dots), and zeta potential (lower panel, bars) of glycerol-transfersomes (green), hyaluronan-transfersomes (blue) and glycerohyaluronan-transfersomes (orange). The same symbols (Δ, □, ϴ, Ω, •, $, ‡, ◊, ∞, #, ?, !, +, %, @, & and £) indicate values that are not statistically different ($p > 0.05$) from the values at the initial time (light green, blue and orange) or among the different groups (cross-comparison) at the same time point (violet). Different symbols indicate significant differences ($p < 0.05$). Mean values ± standard deviations, obtained from at least 3 measurements, are reported. (For interpretation of the references to color in this figure legend, the reader is referred to the Web version of this article.)

was evaluated *in vitro* using vertical Franz cells and calculating the amount of antigen accumulated in the epidermis and dermis at 4 and 8 h after non-occlusive or occlusive (cling film) application (Fig. 4).

After the non-occlusive application of the solution, ovalbumin accumulation was ~6 μg/cm^2 in the epidermis ($p > 0.05$ between the values at 4 and 8 h) and sensibly lower, ~0.5 μg/cm^2 in the dermis ($p > 0.05$ between values at 4 and 8 h). After application of glycerol-transfersomes in the same condition, the deposition was comparable, especially at 4 h. Using hyaluronan-transfersomes and glycerohyaluronan-transfersomes, it was instead higher, ≈10 μg/cm^2 in the epidermis ($p > 0.05$ among the values at 4 and 8 h using the 2 formulations), and ≈1 μg/cm^2 in the dermis ($p > 0.05$ among the values at 4 and 8 h using the 2 formulations), thus indicating that the accumulation of ovalbumin in these skin layers was not influenced by time but only by the formulation used.

By contrast, when ovalbumin formulations were applied under occlusive conditions (cling film), the accumulation was time and formulation-dependent. The solution achieved the lowest accumulation in the epidermis, ≈7 μg/cm2 ($p > 0.05$ between the values at 4 and 8 h). Higher accumulations were achieved by transfersomes, with the highest value, ≈22 μg/cm^2 ($p > 0.05$ versus the values obtained solution and glycerol-transfersomes) provided by hyaluronan-transfersomes at 8 h and glycerohyaluronan-transfersomes at 4 and 8 h. In the dermis, the benefits associated with the occlusive application were significantly visible at 4 and 8 h for all the formulations with respect to the non-occlusive application. Therefore, the occlusive approach significantly enhanced the antigen deposition in this deeper skin layer as the ovalbumin accumulated at 8 h was ~2 μg/cm^2 using the solution, ~3 μg/cm^2 using glycerol-transfersomes, ~5 μg/cm^2 using hyaluronan-transfersomes and ~7 μg/cm^2 using glycerohyaluronan-transfersomes.

Considering the promise demonstrated by the occlusive condition (cling film), the labeled ovalbumin (~330 μg) in solution or encapsulated in enriched transfersomes was loaded into polyvinyl alcohol hydrogel disks (imbibed hydrogel disks) to enable a comparison with the

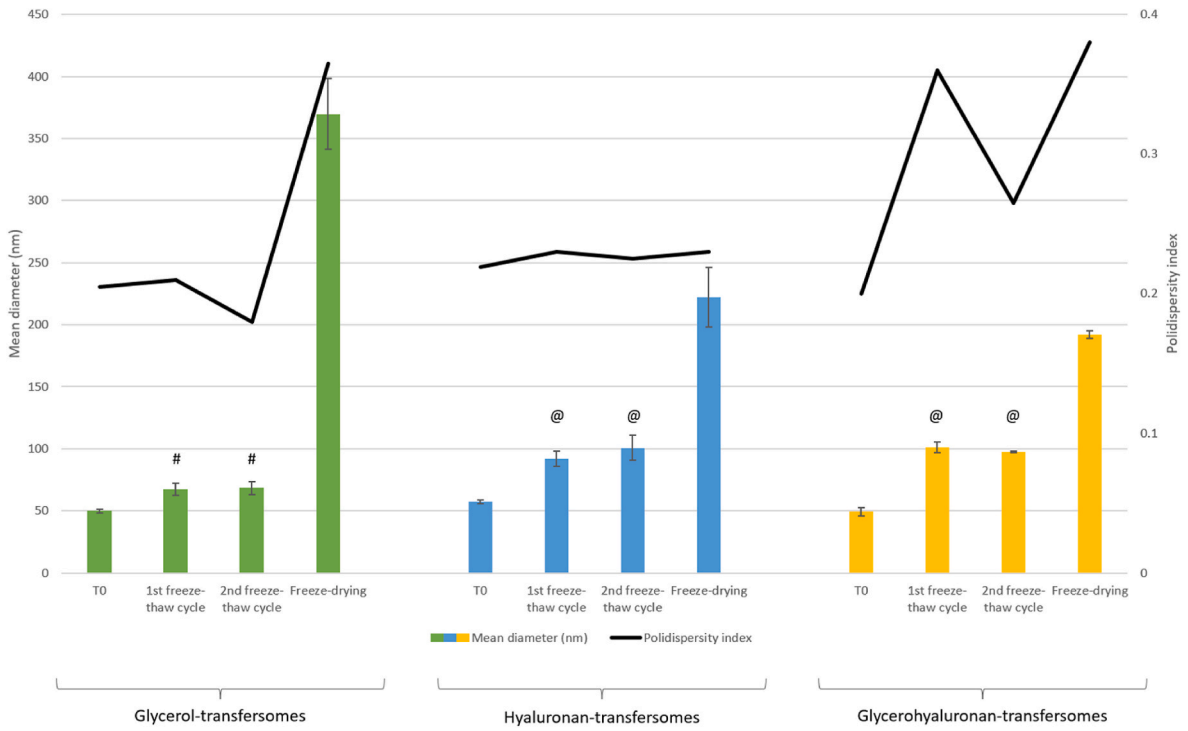

Fig. 3. Mean diameter and polydispersity index of glycerol-transfersomes (green), hyaluronan-transfersomes (blue), and glycerohyaluronan-transfersomes (orange) after the freeze-thawing (2 cycles) and freeze-drying processes. The same symbols (#, @) indicate values that are not statistically different ($p > 0.05$), while different symbols indicate significant differences ($p < 0.05$). Mean values ± standard deviations, obtained from at least 3 measurements, are reported. (For interpretation of the references to color in this figure legend, the reader is referred to the Web version of this article.)

Table 3
Swelling ratio (%) and minimum imbibition time of empty hydrogel disks left swelling in water at different time points (0.5, 1, 2, 3, 4, 6, and 8 h). The same symbols (°, □) indicate values that are not statistically different ($p > 0.05$), while different symbols indicate significant differences ($p < 0.05$). Mean values ± standard deviations, obtained from at least 3 measurements, are reported.

Time (h)	0.5	1	2	3[a]	4	6	8
Swelling ratio (%)	391 ± 2	405 ± 2°	403 ± 2°	420 ± 4□	418 ± 2□	417 ± 2□	421 ± 4□

[a] Attainment of the equilibrium of swelling and the minimum imbibition time.

Table 4
Ovalbumin content (%) of imbibed hydrogel disks after 3 and 12 h of swelling in the presence of ovalbumin in solution or encapsulated in enriched transfersomes. The same symbols (°) indicate values that are not statistically different ($p > 0.05$), while different symbols indicate significant differences ($p < 0.05$). Mean values ± standard deviations, obtained from at least 3 measurements, are reported.

	Ovalbumin content in imbibed hydrogel disks (%)	
	3 h	12 h
Solution	18 ± 2°	19 ± 2°
Glycerol-transfersomes	20 ± 2°	21 ± 2°
Hyaluronan-transfersomes	21 ± 3°	24 ± 4°
Glycerohyaluronan-transfersomes	24 ± 4°	22 ± 2°

occlusive condition after application of the disks for 4 and 8 h on tape-stripped skin (Fig. 5). With respect to the occlusive conditions (cling film), the antigen deposition was greatly improved, at 8 h, by using the imbibed disks likely due to the better adhesion they provide to the skin. The accumulation achieved by the labeled ovalbumin solution imbibed disks was ~9 μg/cm^2 ($p < 0.05$ versus values obtained using the ovalbumin solution with cling film) at 4 h, and it doubled (~18 μg/cm^2) at 8 h, confirming the ability of the hydrogel disks to improve the payload deposition. The antigen deposition was further improved by combining the hydrogel disks and enriched transfersomes. In particular, transfersome-imbibed disks ensured the highest ovalbumin accumulation at 8 h in the epidermis, ≈35 μg/cm^2 ($p > 0.05$ among the values obtained at 8 h using the three transfersome-imbibed disks and $p < 0.05$ versus values obtained at 4 and 8 h applying the solution-imbibed disks). At 4 h instead, the highest deposition was achieved only using glycerohyaluronan-transfersome imbibed disk, and it was ≈23 μg/cm^2 ($p > 0.05$ between the values obtained under occlusive condition and $p < 0.05$ versus the values obtained at 4 h applying the disks imbibed with glycerol-transfersomes and hyaluronan-transfersomes). In the dermis, the highest deposition at 8 h, ≈10 μg/cm^2, was found when using disks imbibed with hyaluronan-transfersomes and glycerohyaluronan-transfersomes ($p > 0.05$ between the 2 values and $p < 0.05$ versus all the other values). By contrast, disks imbibed with either glycerol-transfersomes or ovalbumin solution led to a lower deposition, ≈5 μg/cm^2 ($p < 0.05$ between the 2 values). They were, therefore, less effective than hyaluronan-transfersomes and glycerohyaluronan-transfersomes.

3.5. *In vitro biocompatibility*

The biocompatibility of ovalbumin in solution or encapsulated in enriched transfersomes was tested on the L929 fibroblast cell line (Fig. 6). After 24 h of incubation, the cell viability of all the samples was >60 % and <90 % only using the highest concentration (500 μg/mL of ovalbumin in solution or encapsulated in transfersomes). Using ovalbumin concentrations ≤50 μg/mL, the viability was >90 % and increased in a composition dependant manner (glycerohyaluronan-transfersomes > hyaluronan-transfersomes > glycerol-transfersomes > solution), denoting, in any case, the low toxicity of ovalbumin itself and the beneficial effect provided by its encapsulation into enriched transfersomes.

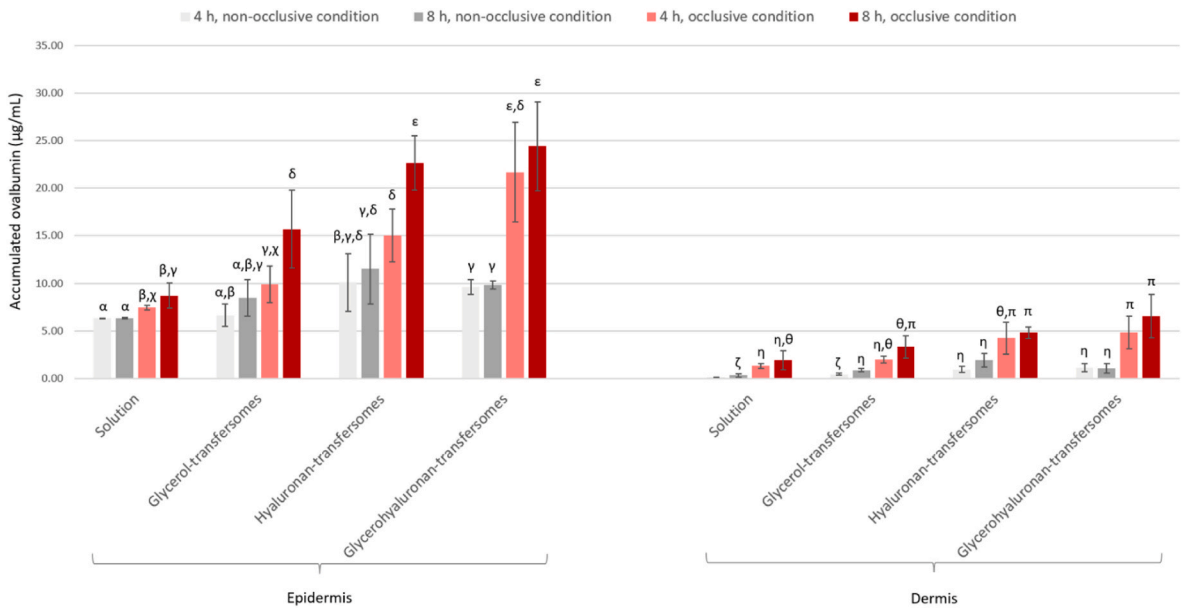

Fig. 4. Amount of ovalbumin (µg/cm^2) accumulated in the epidermis (left) and dermis (right) after application of FITC-ovalbumin, in solution or encapsulated in enriched transfersomes, with cling film (red) or not (grey) at 4 (light colors) and 8 h (dark colors). Same symbols (α, β, γ, χ, δ, ε, ζ, η, θ, π) indicate values that are not statistically different ($p > 0.05$), while different symbols indicate significant differences ($p < 0.05$). Mean values ± standard deviations, obtained from at least 3 measurements, are reported. (For interpretation of the references to color in this figure legend, the reader is referred to the Web version of this article.)

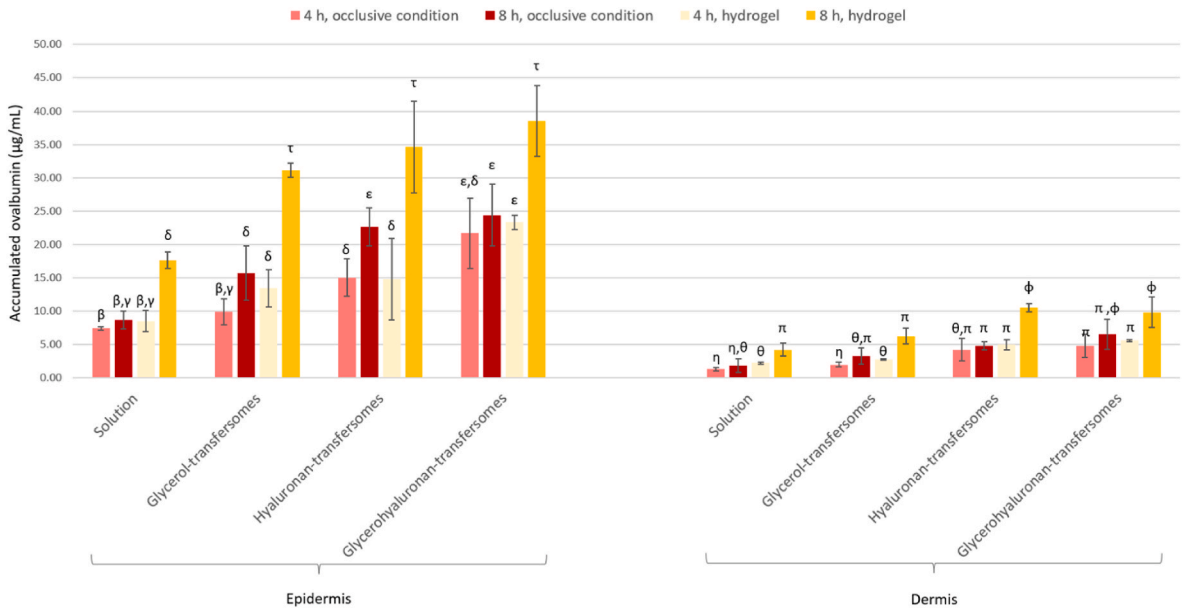

Fig. 5. Amount of ovalbumin (µg/cm^2) accumulated in the epidermis (left) and dermis (right) after application of FITC-ovalbumin in solution or encapsulated in enriched transfersomes, with cling film (red) or hydrogel disks (yellow) at 4 (light colors) and 8 h (dark colors). Same symbols (α, β, γ, δ, τ, η, θ, π, ϕ) indicate values that are not statistically different ($p > 0.05$), while different symbols indicate significant differences ($p < 0.05$). Mean values ± standard deviations, obtained from at least 3 measurements, are reported. (For interpretation of the references to color in this figure legend, the reader is referred to the Web version of this article.)

3.6. *In vitro production of cytokines*

The ability of ovalbumin (5 or 1 µg/mL), in solution or encapsulated in enriched transfersomes, to activate adaptive immunity was evaluated by measuring the production of interleukin-2 by B3Z cells co-cultured with bone marrow-derived dendritic cells preincubated with the described formulations (Fig. 7). The interleukin-2 produced by B3Z co-cultured with dendritic cells-incubated with medium (negative control) was ~10 pg/mL, irrespective to the dose used, indicating the basal production from these cells. When the cells were incubated with ovalbumin (5 or 1 µg/mL), in solution or encapsulated in enriched transfersomes, the value slightly increased up to ~14 pg/mL ($p > 0.05$ versus the control), indicating a minimum but not significant antigen presentation irrespective to the used formulation. Similarly, while the treatment of monocyte-derived macrophages with lipopolysaccharide (positive control), a strong and prototypical inflammatory agent, stimulated the expression of high amount of tumor necrosis factor-α (~4000 pg/mL), the treatment with ovalbumin in solution or encapsulated in enriched transfersomes did not stimulate its production as the measured values were ~50 pg/mL and thus comparable to those found incubating

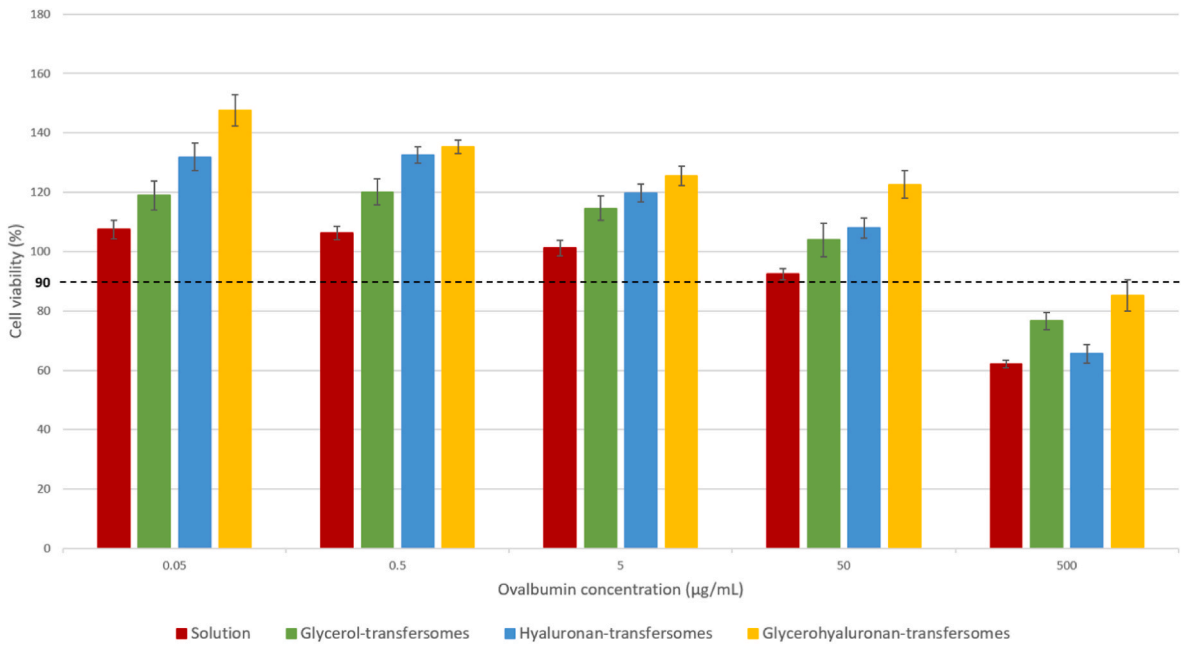

Fig. 6. Cell viability of L929 fibroblasts incubated for 24 h with ovalbumin solution (red), glycerol-transfersomes (green), hyaluronan-transfersomes (blue), and glycerohyaluronan-transfersomes (yellow) diluted with medium to reach 0.05, 0.5, 5, 50 and 500 µg/mL of ovalbumin. Mean values ± standard deviations, obtained from at least 3 measurements, are reported. (For interpretation of the references to color in this figure legend, the reader is referred to the Web version of this article.)

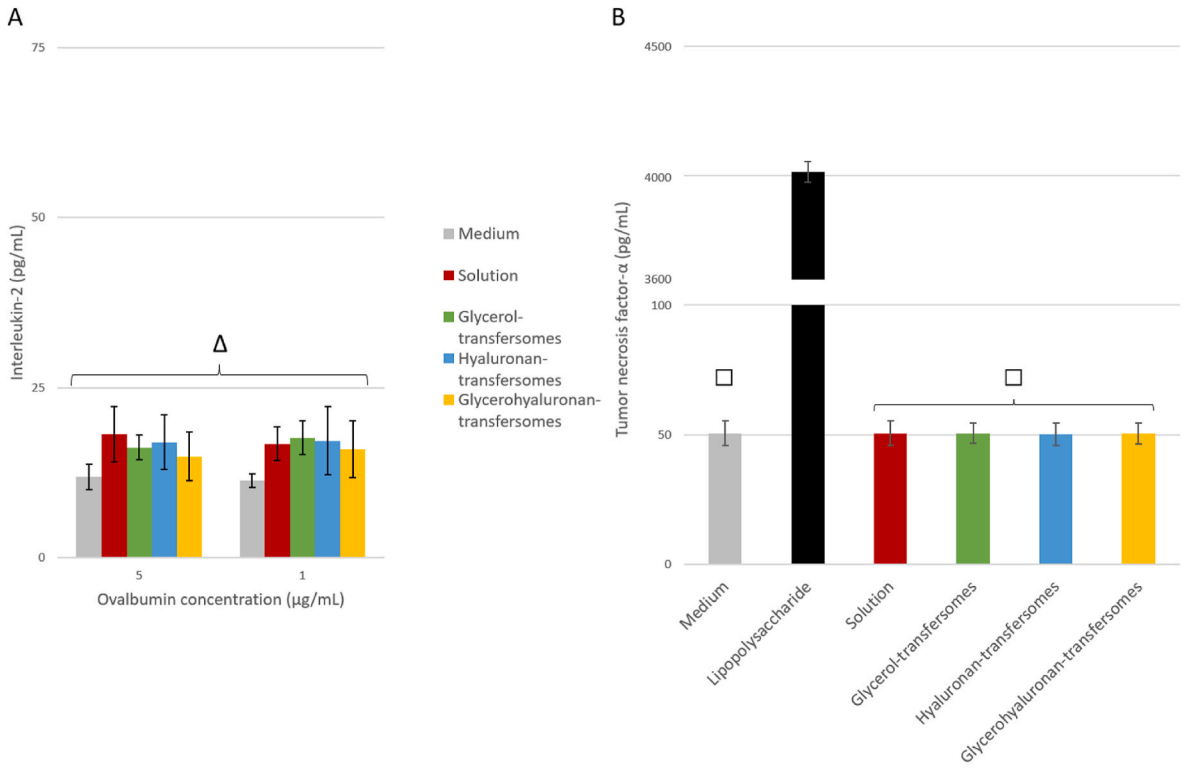

Fig. 7. Production of interleukin-2 by B3Z cells co-cultured with bone marrow-derived dendritic cells (A) and tumor necrosis factor-α by monocyte-derived macrophages (B) after incubation with ovalbumin (5 and 1 µg/mL) in solution (red) or encapsulated in glycerol-transfersomes (green), hyaluronan-transfersomes (blue) and glycerohyaluronan-transfersomes (orange). Medium alone was used as a negative control, while lipopolysaccharide was used as a positive control during the tumor necrosis factor-α detection. The same symbols (Δ, □) indicate values that are not statistically different ($p > 0.05$), while different symbols indicate significant differences ($p < 0.05$). Mean values ± standard deviations are reported. Results are representative of two independent experiments. (For interpretation of the references to color in this figure legend, the reader is referred to the Web version of this article.)

the cells only with medium ($p > 0.05$ among the values obtained with all ovalbumin formulations and negative control, $p < 0.05$ versus positive control). On the whole, despite the good skin penetration performance and high compatibility of the enriched vesicles, the ovalbumin antigen was engulfed and presented at a low extent, and no differences were revealed for either ovalbumin-free or encapsulated, so transfersomes displayed no adjuvanticity at the tested doses.

4. Discussion

This preliminary study aimed to develop and test advanced formulations tailored for antigen accumulation in the skin, combining formulating nanotechnology and physical strategies to overcome the serious hurdles related to the hypodermic injection of vaccines [52]. For this reason, transfersomes, which are ultra-deformable vesicles capable of carrying antigens and drugs across the skin and protecting them from environmental stress, were selected as carriers [53–55]. Lipoid S75, a commercial mixture of phosphatidylcholine, and sodium deoxycholate, a bile salt that acts as an edge-activating surfactant, were used in the preparation due to their skin penetration enhancing properties [56,57]. Furthermore, transfersomes were enriched with glycerol, sodium hyaluronate, or their combination as glycerol-transfersomes, hyaluronan--transfersomes, and glycerohyaluronan-transfersomes are expected to be more effective than unenriched vesicles due to the hydration and lipid fluidization properties provided by these molecules [58,59]. The results achieved by this type of enrichment support findings from other authors and confirm the optimal performance of the resulting vesicles in facilitating payload accumulation in the skin [60–63]. Ovalbumin was used as model antigen at a high dose (5 mg/mL), and no organic solvents were involved during the preparation of vesicles, which was performed by direct sonication, an eco-friendly and one-step method frequently used for drug-loaded phospholipid vesicles variously improved [64–67]. In this respect, this study substantially differs from those performed by other authors, which require instead solvent removal to prevent toxicity [68].

Vesicles prepared with this method were sized <60 nm, thus suitable for skin delivery as a mean diameter <100 nm is recommended to favour skin penetration [69,70]. Their high homogeneity (polydispersity index ~0.2) and negative superficial charge (~30 mV) ensured stability for up to 9 months with no need for stabilizers or preservatives, which are instead used in commercial vaccines [71,72]. This stability was superior to that achieved by Zhang and colleagues, who prepared non-enriched transfersomes from soy phosphatidylcholine, suggesting a beneficial stabilizing role of hyaluronic acid and glycerol in the systems [28].

The ability of the enriched transfersomes to boost the antigen deposition in the skin was evaluated *in vitro*. Only the antigen retained in the skin was quantified as the carriers were meant to be used for local cutaneous immunization [28]. Upon non-occlusive application, the ovalbumin deposition in the epidermis and dermis was slightly improved with respect to the solution but only using hyaluronan-transfersomes and glycerohyaluronan-transfersomes. Using instead occlusive conditions (cling film), the delivery performances of enriched transfersomes were boosted, especially at 8 h, and glycerohyaluronan-transfersomes proved to be the most effective carriers, having the best delivery capabilities. Results agree with what was reported by Ferderber and colleagues, who demonstrated that the amount of drug permeated and retained in the skin can be increased using phosphatidyl choline-based nanocarriers (including transfersomes) under occlusive conditions [73]. The improvement provided by the occlusive application of enriched transfersomes is probably related to the prevention of diffusional water loss from the skin surface, which in turn can alter the stratum corneum function and synergize the moisturizer properties of glycerol and hyaluronic acid as well as the penetration enhancer properties of phosphatidylcholine and sodium deoxycholate, ultimately promoting skin penetration [74–77].

As the occlusive condition achieved by cling film was promising, polyvinyl alcohol hydrogel disks were exploited foreseeing an easier and faster application while keeping the advantages of occlusiveness. Therefore, ad hoc hydrogel disks were successfully prepared by freeze-thawing and freeze-drying cycles and loaded by imbibition with the ovalbumin-encapsulated enriched vesicles or in solution. Disks were imbibed as high as 22 % of the ovalbumin left swelling (300 μL) irrespective of the formulation, thus reaching values commonly reported [78]. Although the dose of ovalbumin applied using transfersomes imbibed disks was lower (~330 μg) than that used with transfersomes applied in an occlusive manner by cling film (500 μg), it is important to highlight that yet at 4 h, disks imbibed with enriched transfersomes were as effective as occlusive conditions in favouring the accumulation of ovalbumin. At 8 h, they were even more effective, emphasizing the suitability of the combination of enriched transfersomes (especially those containing glycerol and hyaluronan) and polyvinyl alcohol disks for antigen deposition in the epidermis and dermis. This effect may be related to the occlusive or semi-occlusive dressing created by the polyvinyl alcohol disks, which grants higher adherence to the skin synergizing with the effect of the vesicle components [79,80]. Results are in fair agreement with those obtained by other authors who exploited hydrogel formulations to promote the penetration of antigenic proteins into the skin or other medications [81,82].

Biocompatibility and immune response were assessed to complete the *in vitro* evaluation of the prepared systems. Biocompatibility was tested using fibroblasts as representative cells of the skin. According to previous studies, all the formulations, including ovalbumin solution, were highly biocompatible (cell viability >100 %) up to 50 μg/mL [83,84]. Since formulations were developed for skin immunization, their ability to stimulate some of the most representative antigen-presenting cells resident in the skin (*i.e.*, dendritic cells and macrophages) was evaluated *in vitro*. Interleukin-2 production was assessed as a measure of effective antigen presentation by ovalbumin-specific T cells in a model of response with dendritic cells, while the production of tumour necrosis factor-α was assessed as a measure of inflammatory response mounted by macrophages. On the bright side, no inflammatory response was detected at any dose tested of ovalbumin in solution or encapsulated in enriched transfersomes, confirming the safety of these carriers for a vaccine formulation. Unfortunately, no *in vitro* immune response stimulation was detected after incubation with ovalbumin in solution or encapsulated in transfersomes. However, as stated by Wang and colleagues, vesicles might be further enriched with molecules having intrinsic or specific adjuvanticity, such as squalene, saponins, or toll-like receptor agonists (e.g., MPLA and CpG ODN), to boost or modulate immune responses providing the same phospholipid vesicles with adjuvanticity [85]. Despite that, the prepared systems, especially glycerohyaluronan-transfersomes imbibed disks, appeared to be optimal carriers capable of modulating and boosting the accumulation of ovalbumin in the skin with respect to the solution, as confirmed by the penetration studies. Consequently, an enhanced activation of the dendritic cells might be expected *in vivo* due to a facilitated exposure to the antigen.

5. Conclusions

In this preliminary study, it was demonstrated that enriched transfersomes (*i.e.*, glycerol-transfersomes, hyaluronan-transfersomes, and glycerohyaluronan-transfersomes) can stably encapsulate ovalbumin, a model antigen, in high dose (5 mg/mL) and can be easily manufactured using an environmentally friendly method involving the direct sonication of the components. All the vesicles had a size suitable for skin penetration (<60 nm), were stable for up to 9 months, and were highly biocompatible (cell viability >100 %). Additionally, they can be used to imbibe dried disks of polyvinyl alcohol hydrogel, creating innovative and advanced systems to facilitate the formulation's application on the skin, anticipating real-life applicability. The prepared imbibed disks, especially those imbibed with glycerohyaluronan-transfersomes, enhanced antigen deposition in the epidermis and dermis, where the

antigen may stimulate an immune response. To the best of our knowledge, this is the first time that these hydrogel disks were imbibed with enriched transfersomes, yielding promising results in antigen accumulation in the skin. Nonetheless, since clinical translation might be challenging, different skin specimens (i.e., human skin) might be used in the attempt to reduce intra-species variability. Moving even further, *in vivo* studies, possibly after association with an adjuvant, will also be essential to support, extend, and confirm skin immunization. All in all, future studies will be essential in confirming the viability of this approach in a real-world context.

CRediT authorship contribution statement

Matteo Aroffu: Writing – original draft, Formal analysis, Data curation, Conceptualization. **Rita Abi Rached:** Formal analysis, Data curation. **Ines Castangia:** Formal analysis, Data curation. **Paola Italiani:** Writing – original draft, Formal analysis, Data curation. **Luciana D'Apice:** Writing – original draft, Formal analysis, Data curation. **Xavier Fernàndez-Busquets:** Formal analysis. **Amparo Nacher:** Formal analysis. **Maria Manconi:** Writing – original draft, Supervision, Methodology, Data curation, Conceptualization. **José Luis Pedraz:** Writing – original draft, Supervision, Data curation, Conceptualization. **Maria Letizia Manca:** Writing – original draft, Supervision, Data curation, Conceptualization.

Declaration of competing interest

The authors declare that they have no known competing financial interests or personal relationships that could have appeared to influence the work reported in this paper.

Appendix A. Supplementary data

Supplementary data to this article can be found online at https://doi.org/10.1016/j.jddst.2024.106399.

Data availability

The authors are unable or have chosen not to specify which data has been used.

References

[1] S. Plotkin, History of vaccination, Proc. Natl. Acad. Sci. U. S. A. 111 (2014) 12283–12287, https://doi.org/10.1073/pnas.1400472111.

[2] M. Lombard, P.P. Pastoret, A.M. Moulin, A brief history of vaccines and vaccination, OIE Revue Scientifique et Technique 26 (2007), https://doi.org/10.20506/rst.26.1.1724.

[3] P.H. Lambert, P.E. Laurent, Intradermal vaccine delivery: will new delivery systems transform vaccine administration? Vaccine. https://doi.org/10.1016/j.vaccine.2008.03.095, 2008.

[4] S. Riedel, Edward Jenner and the history of smallpox and vaccination, Baylor University Medical Center Proceedings 18 (2005), https://doi.org/10.1080/08998280.2005.11928028.

[5] M. Dicko, A.Q.O. Oni, S. Ganivet, S. Kone, L. Pierre, B. Jacquet, Safety of immunization injections in Africa: not simply a problem of logistics, Bull. World Health Organ. 78 (2000).

[6] C. Edens, M.L. Collins, J. Ayers, P.A. Rota, M.R. Prausnitz, Measles vaccination using a microneedle patch, Vaccine 31 (2013), https://doi.org/10.1016/j.vaccine.2012.09.062.

[7] R.M. Jacobson, A. Swan, A. Adegbenro, S.L. Ludington, P.C. Wollan, G.A. Poland, Making vaccines more acceptable - methods to prevent and minimize pain and other common adverse events associated with vaccines, in: Vaccine, 2001, https://doi.org/10.1016/S0264-410X(00)00466-7.

[8] A. Portnoy, S. Ozawa, S. Grewal, B.A. Norman, J. Rajgopal, K.M. Gorham, L. A. Haidari, S.T. Brown, B.Y. Lee, Costs of vaccine programs across 94 low- and middle-income countries, Vaccine 33 (2015), https://doi.org/10.1016/j.vaccine.2014.12.037.

[9] I. Usach, R. Martinez, T. Festini, J.E. Peris, Subcutaneous injection of drugs: Literature review of factors influencing pain sensation at the injection site, Adv. Ther. (2019), https://doi.org/10.1007/s12325-019-01101-6.

[10] G. Orive, A.R. Gascón, R.M. Hernández, A. Domínguez-Gil, J.L. Pedraz, Techniques: new approaches to the delivery of biopharmaceuticals, Trends Pharmacol. Sci. (2004), https://doi.org/10.1016/j.tips.2004.05.006.

[11] L. Engelke, G. Winter, S. Hook, J. Engert, Recent insights into cutaneous immunization: how to vaccinate via the skin, Vaccine 33 (2015), https://doi.org/10.1016/j.vaccine.2015.05.012.

[12] S. Mitragotri, J. Lahann, Materials for drug delivery: innovative solutions to address complex biological hurdles, Adv. Mater. (2012), https://doi.org/10.1002/adma.201202080.

[13] N. Tiwari, E.R. Osorio-Blanco, A. Sonzogni, D. Esporrín-Ubieto, H. Wang, M. Calderón, Nanocarriers for skin applications: where do we stand? Angew. Chem. Int. Ed. (2022) https://doi.org/10.1002/anie.202107960.

[14] H. Daraee, A. Etemadi, M. Kouhi, S. Alimirzalu, A. Akbarzadeh, Application of liposomes in medicine and drug delivery, Artif. Cells, Nanomed. Biotechnol. (2016), https://doi.org/10.3109/21691401.2014.953633.

[15] L. Leserman, Liposomes as protein carriers in immunology, J. Liposome Res. (2004), https://doi.org/10.1081/LPR-200039198.

[16] A. Accardo, G. Morelli, Peptide-targeted liposomes for selective drug delivery: advantages and problematic issues, Biopolymers (2015), https://doi.org/10.1002/BIP.22678.

[17] S.G. Antimisiaris, A. Marazioti, M. Kannavou, E. Natsaridis, F. Gkartziou, G. Kogkos, S. Mourtas, Overcoming barriers by local drug delivery with liposomes, Adv. Drug Deliv. Rev. (2021), https://doi.org/10.1016/j.addr.2021.01.019.

[18] C.T. Inglut, A.J. Sorrin, T. Kuruppu, S. Vig, J. Cicalo, H. Ahmad, H.C. Huang, Immunological and toxicological considerations for the design of liposomes, Nanomaterials (2020), https://doi.org/10.3390/nano10020190.

[19] S. Mallick, J.S. Choi, Liposomes: versatile and biocompatible nanovesicles for efficient biomolecules delivery, J. Nanosci. Nanotechnol. (2014), https://doi.org/10.1166/jnn.2014.9080.

[20] M. Manconi, M.L. Manca, D. Valenti, E. Escribano, H. Hillaireau, A.M. Fadda, E. Fattal, Chitosan and hyaluronan coated liposomes for pulmonary administration of curcumin, Int. J. Pharm. 525 (2017), https://doi.org/10.1016/j.ijpharm.2017.04.044.

[21] M. Moreno-Sastre, M. Pastor, C.J. Salomon, A. Esquisabel, J.L. Pedraz, Pulmonary drug delivery: a review on nanocarriers for antibacterial chemotherapy, J. Antimicrob. Chemother. (2015), https://doi.org/10.1093/jac/dkv192.

[22] Pharmacophore, L. Fritea, S. Cavalu, Formulation, characterization, and advantages of using liposomes in multiple therapies, Simona Ioana Vicaș 11 (2020).

[23] D.S. Tretiakova, E.L. Vodovozova, Liposomes as adjuvants and vaccine delivery systems, Biochem (Mosc) Suppl Ser A Membr Cell Biol (2022), https://doi.org/10.1134/S1990747822020076.

[24] S. Duangjit, Y. Obata, H. Sano, Y. Onuki, P. Opanasopit, T. Ngawhirunpat, T. Miyoshi, S. Kato, K. Takayama, Comparative study of novel ultradeformable liposomes: menthosomes, transfersomes and liposomes for enhancing skin permeation of meloxicam, Biol. Pharm. Bull. 37 (2014), https://doi.org/10.1248/bpb.b13-00576.

[25] M.C. Cristiano, F. Froiio, A. Mancuso, M. Iannone, M. Fresta, S. Fiorito, C. Celia, D. Paolino, In vitro and in vivo trans-epidermal water loss evaluation following topical drug delivery systems application for pharmaceutical analysis, J. Pharm. Biomed. Anal. 186 (2020), https://doi.org/10.1016/j.jpba.2020.113295.

[26] R.K. Tyagi, N.K. Garg, R. Jadon, T. Sahu, O.P. Katare, S.K. Dalai, A. Awasthi, S. K. Marepally, Elastic liposome-mediated transdermal immunization enhanced the immunogenicity of P. falciparum surface antigen, MSP-119. Vaccine 33 (2015), https://doi.org/10.1016/j.vaccine.2015.06.054.

[27] T. Rattanapak, K. Young, T. Rades, S. Hook, Comparative study of liposomes, transfersomes, ethosomes and cubosomes for transcutaneous immunisation: characterisation and in vitro skin penetration, J. Pharm. Pharmacol. 64 (2012), https://doi.org/10.1111/j.2042-7158.2012.01535.x.

[28] Y. Zhang, W. Ng, X. Feng, F. Cao, H. Xu, Lipid vesicular nanocarrier: quick encapsulation efficiency determination and transcutaneous application, Int. J. Pharm. 516 (2017), https://doi.org/10.1016/j.ijpharm.2016.11.011.

[29] I. Castangia, M.L. Manca, A. Catalán-Latorre, A.M. Maccioni, A.M. Fadda, M. Manconi, Phycocyanin-encapsulating hyalurosomes as carrier for skin delivery and protection from oxidative stress damage, J. Mater. Sci. Mater. Med. 27 (2016), https://doi.org/10.1007/s10856-016-5687-4.

[30] M.L. Manca, M. Zaru, M. Manconi, F. Lai, D. Valenti, C. Sinico, A.M. Fadda, Glycerosomes: a new tool for effective dermal and transdermal drug delivery, Int. J. Pharm. 455 (2013), https://doi.org/10.1016/j.ijpharm.2013.07.060.

[31] M.J. Choi, H. Zhai, H. Löffler, F. Dreher, H.I. Maibach, Effect of tape stripping on percutaneous penetration and topical vaccination, Exog. Dermatol. 2 (2003), https://doi.org/10.1159/000078695.

[32] H.I. Maibach, M.J. Choi, H. Löffler, Effect of tape stripping on percutaneous penetration and topical vaccination, in: Percutaneous Absorption, 2021, https://doi.org/10.1201/9780429202971-44.

[33] S. Von Moos, P. Johansen, F. Tay, N. Graf, T.M. Kündig, G. Senti, Comparing safety of abrasion and tape-stripping as skin preparation in allergen-specific epicutaneous immunotherapy, J. Allergy Clin. Immunol. 134 (2014), https://doi.org/10.1016/j.jaci.2014.07.037.

[34] I. Castangia, F. Fulgheri, F.J. Leyva-Jimenez, M.E. Alañón, M. de la L. Cádiz-Gurrea, F. Marongiu, M.C. Meloni, M. Aroffu, M. Perra, M. Allaw, R. Abi Rached, R. Oliver-Simancas, E. Escribano Ferrer, F. Asunis, M.L. Manca, M. Manconi, From grape by-products to enriched yogurt containing pomace extract loaded in nanotechnological nutriosomes tailored for promoting gastro-intestinal wellness, Antioxidants 12 (2023), https://doi.org/10.3390/antiox12061285.

[35] L. Román-Álamo, M. Allaw, Y. Avalos-Padilla, M.L. Manca, M. Manconi, F. Fulgheri, J. Fernández-Lajo, L. Rivas, J.A. Vázquez, J.E. Peris, X. Roca-Geronès, S. Poonlaphdecha, M.M. Alcover, R. Fisa, C. Riera, X. Fernàndez-Busquets, In vitro evaluation of aerosol therapy with pentamidine-loaded liposomes coated with chondroitin sulfate or heparin for the treatment of leishmaniasis, Pharmaceutics 15 (2023), https://doi.org/10.3390/pharmaceutics15041163.
[36] C. Loira-Pastoriza, K. Vanvarenberg, B. Ucakar, M. Machado Franco, A. Staub, M. Lemaire, J.C. Renauld, R. Vanbever, Encapsulation of a CpG oligonucleotide in cationic liposomes enhances its local antitumor activity following pulmonary delivery in a murine model of metastatic lung cancer, Int. J. Pharm. 600 (2021), https://doi.org/10.1016/j.ijpharm.2021.120504.
[37] I. Castangia, M. Aroffu, M. Allaw, M. Perra, B. Baroli, I. Usach, J.E. Peris, D. Valenti, O. Diez-Sales, A.R. Sauri, A. Nacher, X. Fernàndez-Busquets, M. Manconi, M.L. Manca, Beclomethasone loaded liposomes enriched with mucin: a suitable approach for the control of skin disorders, Biomed. Pharmacother. 177 (2024) 116998, https://doi.org/10.1016/j.biopha.2024.116998.
[38] S. Garg, P. Patel, G. Das Gupta, B. Das Kurmi, Pharmaceutical applications and advances with zetasizer: an essential analytical tool for size and zeta potential analysis, Micro Nanosyst. 16 (2024) 139–154, https://doi.org/10.2174/0118764029301470240603051432.
[39] M. Allaw, M.L. Manca, J.C. Gómez-Fernández, J.L. Pedraz, M.C. Terencio, O. D. Sales, A. Nacher, M. Manconi, Oleuropein multicompartment nanovesicles enriched with collagen as A natural strategy for the treatment of skin wounds connected with oxidative stress, Nanomedicine 16 (2021) 2363–2376, https://doi.org/10.2217/nnm-2021-0197.
[40] M. Laura Soriano Pérez, I. Montironi, J. Alejandro Funes, C. Margineda, N. Campra, L. Noelia Cariddi, J. José Garrido, M. Molina, F. Alustiza, Nanogel-Mediated antigen delivery: biocompatibility, immunogenicity, and potential for tailored vaccine design across species, Vaccine 42 (2024) 3721–3732, https://doi.org/10.1016/j.vaccine.2024.04.086.
[41] A. Ahsan, M.A. Farooq, Therapeutic potential of green synthesized silver nanoparticles loaded PVA hydrogel patches for wound healing, J. Drug Deliv. Sci. Technol. 54 (2019), https://doi.org/10.1016/j.jddst.2019.101308.
[42] S. Ahmed, S. Fujita, K. Matsumura, A freeze-concentration and polyampholyte-modified liposome-based antigen-delivery system for effective immunotherapy, Adv. Healthcare Mater. 6 (2017), https://doi.org/10.1002/adhm.201700207.
[43] K. Moulaoui, C. Caddeo, M.L. Manca, I. Castangia, D. Valenti, E. Escribano, D. Atmani, A.M. Fadda, M. Manconi, Identification and nanoentrapment of polyphenolic phytocomplex from Fraxinus angustifolia: in vitro and in vivo wound healing potential, Eur. J. Med. Chem. 89 (2015), https://doi.org/10.1016/j.ejmech.2014.10.047.
[44] A.C. Ayub, A.D.M. Gomes, M.V.C. Lima, C.D. Vianna-Soares, L.A.M. Ferreira, Topical delivery of fluconazole: in vitro skin penetration and permeation using emulsions as dosage forms, Drug Dev. Ind. Pharm. 33 (2007), https://doi.org/10.1080/03639040600829989.
[45] A. da S. Meira, A.P. Battistel, H.F. Teixeira, N.M. Volpato, Evaluation of porcine skin layers separation methods, freezing storage and anatomical site in in vitro percutaneous absorption studies using penciclovir formulations, J. Drug Deliv. Sci. Technol. 60 (2020), https://doi.org/10.1016/j.jddst.2020.101926.
[46] F. Miller, U. Hinze, B. Chichkov, W. Leibold, T. Lenarz, G. Paasche, Validation of eGFP fluorescence intensity for testing in vitro cytotoxicity according to ISO 10993-5, J. Biomed. Mater. Res. B Appl. Biomater. 105 (2017), https://doi.org/10.1002/jbm.b.33602.
[47] M. Kamalov, H. Kählig, C. Rentenberger, A.R.M. Müllner, H. Peterlik, C.F. W. Becker, Ovalbumin epitope SIINFEKL self-assembles into a supramolecular hydrogel, Sci. Rep. 9 (2019), https://doi.org/10.1038/s41598-019-39148-8.
[48] D.C.F. Wieland, P. Degen, T. Zander, S. Gayer, A. Raj, J. An, A. Dėdinaitė, P. Claesson, R. Willumeit-Römer, Structure of DPPC–hyaluronan interfacial layers – effects of molecular weight and ion composition, Soft Matter 12 (2016) 729–740, https://doi.org/10.1039/C5SM01708D.
[49] M.L. Manca, M. Manconi, M. Zaru, D. Valenti, J.E. Peris, P. Matricardi, A. M. Maccioni, A.M. Fadda, Glycerosomes: investigation of role of 1,2-dimyristoyl-sn-glycero-3-phosphatidycholine (DMPC) on the assembling and skin delivery performances, Int. J. Pharm. 532 (2017), https://doi.org/10.1016/j.ijpharm.2017.09.026.
[50] S. Bhattacharjee, DLS and zeta potential – what they are and what they are not? J. Contr. Release 235 (2016) 337–351, https://doi.org/10.1016/j.jconrel.2016.06.017.
[51] M. Danaei, M. Dehghankhold, S. Ataei, F. Hasanzadeh Davarani, R. Javanmard, A. Dokhani, S. Khorasani, M.R. Mozafari, Impact of particle size and polydispersity index on the clinical applications of lipidic nanocarrier systems, Pharmaceutics (2018), https://doi.org/10.3390/pharmaceutics10020057.
[52] M.J. Papania, D. Zehrung, C. Jarrahian, Technologies to improve immunization, in: Plotkin's Vaccines, 2017, https://doi.org/10.1016/B978-0-323-35761-6.00068-7.
[53] M.W. Akram, H. Jamshaid, F.U. Rehman, M. Zaeem, J. zeb Khan, A. Zeb, Transfersomes: a revolutionary nanosystem for efficient transdermal drug delivery, AAPS PharmSciTech (2022), https://doi.org/10.1208/s12249-021-02166-9.
[54] R. Gupta, A. Kumar, Transfersomes: the ultra-deformable carrier system for non-invasive delivery of drug, Curr. Drug Deliv. 18 (2020), https://doi.org/10.2174/1567201817666200804105416.
[55] Simrah, A. Hafeez, S.A. Usmani, M.P. Izhar, Transfersome, an ultra-deformable lipid-based drug nanocarrier: an updated review with therapeutic applications, Naunyn-Schmiedeberg's Arch. Pharmacol. (2023), https://doi.org/10.1007/s00210-023-02670-8.
[56] G.M. El Zaafarany, G.A.S. Awad, S.M. Holayel, N.D. Mortada, Role of edge activators and surface charge in developing ultradeformable vesicles with enhanced skin delivery, Int. J. Pharm. 397 (2010), https://doi.org/10.1016/j.ijpharm.2010.06.034.
[57] M. Ghadiri, P.M. Young, D. Traini, Strategies to enhance drug absorption via nasal and pulmonary routes, Pharmaceutics (2019), https://doi.org/10.3390/pharmaceutics11030113.
[58] D. Rani, V. Sharma, P. Singh, R. Singh, Glycerosomes: a novel vesicular drug delivery system, Res. J. Pharm. Technol. (2022), https://doi.org/10.52711/0974-360X.2022.00154.
[59] M. Witting, A. Boreham, R. Brodwolf, K. Vávrová, U. Alexiev, W. Friess, S. Hedtrich, Interactions of hyaluronic acid with the skin and implications for the dermal delivery of biomacromolecules, Mol. Pharm. 12 (2015), https://doi.org/10.1021/mp500676e.
[60] I. Castangia, M.L. Manca, M. Allaw, J. Hellström, D. Granato, M. Manconi, Jabuticaba (Myrciaria jaboticaba) peel as a sustainable source of anthocyanins and ellagitannins delivered by phospholipid vesicles for alleviating oxidative stress in human keratinocytes, Molecules 26 (2021), https://doi.org/10.3390/molecules26216697.
[61] M. Firoznezhad, I. Castangia, C.I.G. Tuberoso, F. Cottiglia, F. Marongiu, M. Porceddu, I. Usach, E. Escribano-Ferrer, M.L. Manca, M. Manconi, Formulation and in vitro efficacy assessment of teucrium marum extract loading hyalurosomes enriched with tween 80 and glycerol, Nanomaterials 12 (2022), https://doi.org/10.3390/nano12071096.
[62] M.L. Manca, M. Firoznezhad, C. Caddeo, F. Marongiu, E. Escribano-Ferrer, G. Sarais, J.E. Peris, I. Usach, M. Zaru, M. Manconi, A.M. Fadda, Phytocomplexes extracted from grape seeds and stalks delivered in phospholipid vesicles tailored for the treatment of skin damages, Ind. Crops Prod. 128 (2019), https://doi.org/10.1016/j.indcrop.2018.11.052.
[63] R. Sklenarova, M. Allaw, M. Perra, I. Castangia, J. Frankova, J. Luis Pedraz, M. Letizia Manca, M. Manconi, Co-delivering of oleuropein and lentisk oil in phospholipid vesicles as an effective approach to modulate oxidative stress, cytokine secretion and promote skin regeneration, Eur. J. Pharm. Biopharm. 185 (2023), https://doi.org/10.1016/j.ejpb.2023.02.018.
[64] I. Castangia, M.L. Manca, C. Caddeo, G. Bacchetta, R. Pons, D. Demurtas, O. Diez-Sales, A.M. Fadda, M. Manconi, Santosomes as natural and efficient carriers for the improvement of phycocyanin reepithelising ability in vitro and in vivo, Eur. J. Pharm. Biopharm. 103 (2016), https://doi.org/10.1016/j.ejpb.2016.03.033.
[65] F. Fulgheri, M. Aroffu, M. Ramírez, L. Román-Álamo, J.E. Peris, I. Usach, A. Nacher, M. Manconi, X. Fernàndez-Busquets, M.L. Manca, Curcumin or quercetin loaded nutriosomes as oral adjuvants for malaria infections, Int. J. Pharm. 643 (2023), https://doi.org/10.1016/j.ijpharm.2023.123195.
[66] M. Manconi, M. Rezvani, M.L. Manca, E. Escribano-Ferrer, S. Fais, G. Orrù, T. Lammers, F. Asunis, A. Muntoni, D. Spiga, G. De Gioannis, Bridging biotechnology and nanomedicine to produce biogreen whey-nanovesicles for intestinal health promotion, Int. J. Pharm. 633 (2023), https://doi.org/10.1016/j.ijpharm.2023.122631.
[67] M. Perra, L. Fancello, I. Castangia, M. Allaw, E. Escribano-Ferrer, J.E. Peris, I. Usach, M.L. Manca, I.K. Koycheva, M.I. Georgiev, M. Manconi, Formulation and testing of antioxidant and protective effect of hyalurosomes loading extract rich in rosmarinic acid biotechnologically produced from lavandula angustifolia miller, Molecules 27 (2022), https://doi.org/10.3390/molecules27082423.
[68] M. Aroffu, M.L. Manca, J.L. Pedraz, M. Manconi, Liposome-based vaccines for minimally or noninvasive administration: an update on current advancements, Expet Opin. Drug Deliv. 20 (2023) 1573–1593, https://doi.org/10.1080/17425247.2023.2288856.
[69] A.C. Carita, J.O. Eloy, M. Chorilli, R.J. Lee, G.R. Leonardi, Recent advances and perspectives in liposomes for cutaneous drug delivery, Curr. Med. Chem. 25 (2017), https://doi.org/10.2174/0929867324666171009120154.
[70] R. Touti, M. Noun, F. Guimberteau, S. Lecomte, C. Faure, What is the fate of multilamellar liposomes of controlled size, charge and elasticity in artificial and animal skin? Eur. J. Pharm. Biopharm. 151 (2020) https://doi.org/10.1016/j.ejpb.2020.03.017.
[71] J. Domachowske, Vaccine additives and excipients, in: Vaccines, 2021, https://doi.org/10.1007/978-3-030-58414-6_4.
[72] R. Taléns-Visconti, M. Perra, A. Ruiz-Saurí, A. Nácher, New vehiculation systems of mometasone furoate for the treatment of inflammatory skin diseases, Pharmaceutics 14 (2022), https://doi.org/10.3390/pharmaceutics14122558.
[73] K. Ferderber, S. Hook, T. Rades, Phosphatidyl choline-based colloidal systems for dermal and transdermal drug delivery, J. Liposome Res. 19 (2009), https://doi.org/10.3109/08982100902814006.
[74] N.I.W. Azelee, A.N.M. Ramli, N.H.A. Manas, N. Salamun, R.C. Man, H. El Enshasy, Glycerol in food, cosmetics and pharmaceutical industries: basics and new applications, International Journal of Scientific and Technology Research 8 (2019).
[75] C. Kim, J. Shim, S. Han, I. Chang, The skin-permeation-enhancing effect of phosphatidylcholine: caffeine as a model active ingredient, J. Cosmet. Sci. 53 (2002).
[76] C. Ni, Zijun Zhang, Y. Wang, Zhenhai Zhang, X. Guo, H. Lv, Hyaluronic acid and HA-modified cationic liposomes for promoting skin penetration and retention, J. Contr. Release 357 (2023), https://doi.org/10.1016/j.jconrel.2023.03.049.
[77] H. Zhai, H.I. Maibach, Occlusion vs. skin barrier function, Skin Res. Technol. (2002), https://doi.org/10.1046/j.0909-752x.2001.10311.x.
[78] A. Ahsan, W.X. Tian, M.A. Farooq, D.H. Khan, An overview of hydrogels and their role in transdermal drug delivery, International Journal of Polymeric Materials and Polymeric Biomaterials (2021), https://doi.org/10.1080/00914037.2020.1740989.

[79] T. Lima, P. de L. de, M.F. Passos, Skin wounds, the healing process, and hydrogel-based wound dressings: a short review, J. Biomater. Sci. Polym. Ed. (2021), https://doi.org/10.1080/09205063.2021.1946461.
[80] S. Napavichayanun, W. Bonani, Y. Yang, A. Motta, P. Aramwit, Fibroin and polyvinyl alcohol hydrogel wound dressing containing silk sericin prepared using high-pressure carbon dioxide, Adv. Wound Care 8 (2019), https://doi.org/10.1089/wound.2018.0856.
[81] P. Basu, N. Saha, T. Saha, P. Saha, Polymeric hydrogel based systems for vaccine delivery: a review, Polymer (Guildf) (2021), https://doi.org/10.1016/j.polymer.2021.124088.
[82] D.R. De Araújo, D.C. Da Silva, R.M. Barbosa, M. Franz-Montan, C.M. Cereda, C. Padula, P. Santi, E. De Paula, Strategies for delivering local anesthetics to the skin: focus on liposomes, solid lipid nanoparticles, hydrogels and patches, Expet Opin. Drug Deliv. (2013), https://doi.org/10.1517/17425247.2013.828031.
[83] M.T. Hussain, M. Tiboni, Y. Perrie, L. Casettari, Microfluidic production of protein loaded chimeric stealth liposomes, Int. J. Pharm. 590 (2020), https://doi.org/10.1016/j.ijpharm.2020.119955.
[84] K. Taguchi, Y. Okamoto, K. Matsumoto, M. Otagiri, V.T.G. Chuang, When albumin meets liposomes: a feasible drug carrier for biomedical applications, Pharmaceuticals (2021), https://doi.org/10.3390/ph14040296.
[85] N. Wang, M. Chen, T. Wang, Liposomes used as a vaccine adjuvant-delivery system: from basics to clinical immunization, J. Contr. Release (2019), https://doi.org/10.1016/j.jconrel.2019.04.025.